Published OnlineFirst January 17, 2012; DOI:10.1158/1535-7163.MCT-11-0826

Molecular Cancer Therapeutics

Next Generation Sequencing of Prostate Cancer from a Patient Identifies a Deficiency of Methylthioadenosine Phosphorylase, an Exploitable Tumor Target

Colin C. Collins, Stanislav V. Volik, Anna V. Lapuk, et al.

Mol Cancer Ther 2012;11:775-783. Published OnlineFirst January 17, 2012.

Published OnlineFirst January 17, 2012; DOI:10.1158/1535-7163.MCT-11-0826

Molecular Cancer Therapeutics

Next Generation Sequencing of Prostate Cancer from a Patient Identifies a Deficiency of Methylthioadenosine Phosphorylase, an Exploitable Tumor Target

Colin C. Collins[1], Stanislav V. Volik[1], Anna V. Lapuk[1], Yuwei Wang[1,2], Peter W. Gout[2], Chunxiao Wu[1], Hui Xue[1,2], Hongwei Cheng[1,2], Anne Haegert[1], Robert H. Bell[1], Sonal Brahmbhatt[1], Shawn Anderson[1], Ladan Fazli[1], Antonio Hurtado-Coll[1], Mark A. Rubin[3], Francesca Demichelis[3], Himisha Beltran[3], Martin Hirst[2], Marco Marra[2], Christopher A. Maher[4], Arul M. Chinnaiyan[4], Martin Gleave[1], Joseph R. Bertino[5], Martin Lubin[6], and Yuzhuo Wang[1,2]

Abstract

Castrate-resistant prostate cancer (CRPC) and neuroendocrine carcinoma of the prostate are invariably fatal diseases for which only palliative therapies exist. As part of a prostate tumor sequencing program, a patient tumor was analyzed using Illumina genome sequencing and a matched renal capsule tumor xenograft was generated. Both tumor and xenograft had a homozygous 9p21 deletion spanning the *MTAP*, *CDKN2*, and *ARF* genes. It is rare for this deletion to occur in primary prostate tumors, yet approximately 10% express decreased levels of methylthioadenosine phosphorylase (MTAP) mRNA. Decreased *MTAP* expression is a prognosticator for poor outcome. Moreover, it seems that this deletion is more common in CRPC than in primary prostate cancer. We show for the first time that treatment with methylthioadenosine and high dose 6-thioguanine causes marked inhibition of a patient-derived neuroendocrine xenograft growth while protecting the host from 6-thioguanine toxicity. This therapeutic approach can be applied to other MTAP-deficient human cancers as deletion or hypermethylation of the *MTAP* gene occurs in a broad spectrum of tumors at high frequency. The combination of genome sequencing and patient-derived xenografts can identify candidate therapeutic agents and evaluate them for personalized oncology. *Mol Cancer Ther; 11(3); 775–83. ©2012 AACR.*

Introduction

Annually, in North America, prostate cancer is diagnosed in 220,000 men and kills approximately 35,000, making it the second leading cause of cancer-related deaths for men. It is estimated that one in 6 men will develop the disease in their lifetime. Prostate cancer grows most commonly as an adenocarcinoma with varying degrees of neuroendocrine differentiation. Focal neuroendocrine differentiation is observed at all stages of prostate cancer to various extents (30%–100%; ref. 1). Pure neuroendocrine prostate cancers are rare but extraordinarily aggressive, resistant to therapy, and associated with poor patient survival (2, 3). Small cell carcinoma of the prostate is a pathologic subtype of prostate cancer with unique clinical features and accounts for no more than 1% of all the prostatic malignancies. Typically they are discovered at an advanced stage or as recurrences of castration-resistant adenocarcinoma following treatment with hormonal therapy (4–8). In contrast to androgen-dependent adenocarcinoma of the prostate, small cell carcinomas do not usually express the androgen receptor (AR) or prostate-specific antigen (PSA) but do frequently express neuroendocrine markers such as chromogranin A, synaptophysin, CD56, and neuron-specific enolase (9, 10). Because neuroendocrine prostate cancers do not express AR, they are not responsive to antiandrogens, rendering mainstream therapies for prostate cancer ineffective and making chemotherapy the dominant treatment option. Unfortunately, responses are short lived and neuroendocrine prostate cancer is invariably fatal (11, 12), making identification of novel therapeutic targets and more effective therapies critical.

Whole-genome sequencing of prostate tumors and patient-derived prostate tumor xenografts identified one patient with metastatic neuroendocrine prostate cancer that had a homozygous deletion of the *methylthioadenosine phosphorylase* (*MTAP*) gene and thus presented an

Authors' Affiliations: [1]Vancouver Prostate Centre & Department of Urologic Sciences, University of British Columbia; [2]BC Cancer Research Centre, BC Cancer Agency, Vancouver, British Columbia, Canada; [3]Weill Cornell Medical College, New York; [4]Department of Pathology, University of Michigan, Ann Arbor, Michigan; [5]Cancer Institute of New Jersey, New Brunswick, New Jersey; and [6]Dartmouth Medical School, Hanover, New Hampshire

Note: Supplementary material for this article is available at Molecular Cancer Therapeutics Online (http://mct.aacrjournals.org/).

Corresponding Author: Colin C. Collins, Vancouver Prostate Centre, 2660 Oak Street, Vancouver, British Columbia, Canada V6H 3Z6. Phone: 604-779-9287; Fax: 604-875-5654; E-mail: ccollins@prostatecentre.com

doi: 10.1158/1535-7163.MCT-11-0826

Published OnlineFirst January 17, 2012; DOI:10.1158/1535-7163.MCT-11-0826

opportunity to test a recently proposed treatment strategy that had been successfully used with a human T-cell leukemia xenograft (13).

The *MTAP* gene encodes an enzyme that plays a major role in the metabolism of polyamines, compounds important in the proliferation and development of mammalian cells (14–18); there is considerable evidence that *MTAP* also functions as a tumor suppressor (19, 20). Deletions of *MTAP* frequently occur in conjunction with deletion of cyclin-dependent kinase inhibitor 2A (*CDKN2A*), a gene that encodes, via alternative processing, the tumor suppressor proteins $p16^{ink4A}$ and $p14^{ARF}$, important in the regulation of *p53* and *Rb* pathways (21). Consistent with their regulatory functions, *MTAP* and *CDKN2A* genes/proteins are frequently found to be codeleted in a wide range of cancers, including breast, endometrial, non–small cell lung and pancreatic cancers, gliomas, mesotheliomas, osteosarcomas, soft tissue sarcomas, and T-cell acute leukemias at frequencies ranging from 10% to 75% (reviewed in ref. 13). In mantle cell lymphomas, mesotheliomas, and gastrointestinal stromal cancers the *MTAP-CDKN2A* deletion is correlated with poor patient survival (14, 16, 22). The *MTAP* gene can also be silenced epigenetically, by promoter methylation, in malignant melanoma (23).

Over the past 30 years, several strategies to treat MTAP-deficient tumors have been suggested (13). Because *in vitro* evidence showed that MTAP-deficient tumors have increased sensitivity to inhibitors of *de novo* purine biosynthesis, one such inhibitor—L-alanosine—was tested in a broad clinical trial. This trial failed to show any objective response (13, 24). In a more recent proposal, 5′-deoxy-5′-methylthioadenosine (MTA), the natural substrate of the enzyme MTAP, is administered with an antimetabolite—either an adenine analogue, such as 2,6-diaminopurine, or a pyrimidine analogue, such as the clinically approved drug 5-fluorouracil, or, as used in the present study, another clinically approved drug, the guanine analogue 6-thioguanine (6-TG; ref. 15). These analogues are phosphoribosylated in cells to toxic nucleotides with 5-phosphoribosyl-1-pyrophosphate (PRPP) as the donor of the phosphoribosyl group. In normal, MTAP-containing cells, MTA is cleaved by MTAP to 5-methylthioribose-1-phosphate (which is further metabolized to methionine) and to adenine. The MTA-derived adenine is phosphoribosylated by adenine phosphoribosyltransferase (APRT) to form AMP, consuming PRPP, and hence, competitively inhibiting phosphoribosylation of 6-TG to a toxic nucleotide, thus protecting the normal cells. In MTAP-deficient tumor cells, adenine cannot be generated from the supplied MTA and the activation of 6-TG to its toxic nucleotide is not inhibited, resulting in toxicity to the tumor cells.

The combination of MTA and 6-TG was shown to permit administration of extremely high—even lethal—doses of 6-TG, to treat an MTAP-deficient human T-cell leukemia CCRF-CEM xenograft, whereas the normal host tissues of the mouse, which all have MTAP, were protected (13). This demonstration of successful application of the strategy in treating a hematologic tumor suggested that MTA, combined with high dose 6-TG, might also be applicable to solid tumors. Such solid tumors have not been shown to respond to 6-TG, in a clinical setting, because the dose of permissible 6-TG has been limited by toxicity, primarily to bone marrow. The treatment strategy described here may have application to many different MTAP-deficient solid tumors.

We now report successful application of this approach to a subrenal capsule xenograft generated from a patient's neuroendocrine prostate tumor that was shown to have an *MTAP-CDKN2A* deletion via massively parallel genome sequencing [(massively parallel sequencing (MPS)].

Materials and Methods

Materials and animals

Chemicals, stains, solvents, and solutions were obtained from Sigma-Aldrich Canada Ltd., unless otherwise indicated. Male 6- to 8-week-old nonobese diabetic/severe combined immunodeficient (NOD/SCID) mice were bred by the BC Cancer Research Centre Animal Resource Centre, BC Cancer Agency, Vancouver, British Columbia, Canada. Mice were housed in groups of 3 in microisolators with free access to food and water and their health was monitored daily. Prostate cancer specimens were obtained at the Vancouver Prostate Centre, Vancouver General Hospital, with the patient's written and informed consent. The nature and consequences of the studies were explained. All experimental protocols were approved by the University of British Columbia Animal Care Committee. Ethical approval was provided by the University of British Columbia (Vancouver, British Columbia, Canada)—British Columbia Cancer Agency Research Ethics Board (UBC BCCA REB #H04-60131).

Development of the LTL352 xenograft line: Use in 6-TG + MTA efficacy studies

Subrenal capsule xenografts were established from the patient's NE urethral metastatic tissue using routine methodology previously described (25). Briefly, fresh tumor tissue was collected and cut into $1 \times 2 \times 3$ mm^3 pieces and then grafted under the renal capsules of 6 male NOD/SCID mice. Some of the rapidly growing grafts were maintained for up to 5 transplant generations by serial subrenal capsule transplantation into male NOD/SCID mice. A transplantable tumor tissue line, designated LTL352, was stored frozen with dimethyl sulfoxide (DMSO) in liquid nitrogen for further use. For efficacy studies, LTL352 tissue was resurrected from liquid nitrogen storage and pieces of tissue were grafted into the subrenal capsule graft site of NOD/SCID mice to increase the amount of cancer tissue. After 2 months, the tissues were harvested and cut into small pieces ($1 \times 2 \times 3$ mm^3) and then grafted subcutaneously into 19 male NOD/SCID mice. After 5 weeks (to allow enlargement of the grafts >100 mm^3), the 19 mice were randomly distributed into 3

Published OnlineFirst January 17, 2012; DOI:10.1158/1535-7163.MCT-11-0826

groups and treated (intraperitoneally) on days 1, 5, and 9 with: (i) 6-TG, (ii) 6-TG + MTA, and (iii) similar volumes of saline (controls). Tumor sizes were measured with calipers (mm) on days 1, 5, 9, and 12; all xenografts were harvested on day 12.

Histology and immunohistochemistry

Human prostate tissue samples and xenograft tissues were fixed in 10% neutral-buffered formalin and embedded in paraffin. Serial sections (5-μm thick) were cut on a microtome, mounted on glass slides, dewaxed in Histo-Clear (National Diagnostic) and then hydrated in graded alcohol solutions and distilled water. One slide was stained with hematoxylin and eosin (H&E) for histologic characterization and adjacent sections of each tissue sample were used for immunohistochemical staining. For immunohistochemical staining, endogenous peroxidase activity was blocked with 0.5% hydrogen peroxide in methanol for 10 minutes followed by washing with PBS (pH 7.4). Blocking solution (ImmunoVision Technology) was applied to the sections for 60 minutes to block nonspecific sites. The sections were then incubated with primary antibodies overnight at 4°C. Following incubation with the primary antibodies, sections were washed with PBS and incubated for 30 minutes at room temperature with the appropriate biotinylated secondary antibodies and then incubated with avidin–biotin complex (Vector Laboratories) for 30 minutes at room temperature. Immunoreactivity was visualized with 3,3′-diaminobenzidine (DAB) reaction. Sections were counterstained with hematoxylin and dehydrated in graded alcohols. Primary antibodies used included rabbit anti-synaptophysin (Abcam Inc.); mouse anti-Ki-67 (DAKO; 1:50); rabbit anti-caspase-3 (Cell Signaling; 1:100); mouse antihuman P63 monoclonal, and rabbit antihuman AR polyclonal antibody (Santa Cruz Biotechnology). Control sections were processed in parallel with mouse or rabbit nonimmune IgG (Dako) used at the same concentrations as the primary antibodies.

Quantification of caspase-3–positive cells

For quantification of caspase-3 immunostaining of cells, 5 randomly selected high-power (×400) images from each graft were captured using an AxioCam HRCCD mounted on an Axioplan 2 microscope, with Axiovision 3.1 software (Carl Zeiss). The percentages of caspase-3–positive cells were calculated using the formula: percentage = number of positive cells × 100/number of total cells. Viable tumor areas of the treated and control groups were averaged and presented as means ± SD. *P* values were calculated with a permutation test of the means. Caspase-3 percentages are presented as means ± SD and analyzed by the Student *t* test. Results with *P* values less than 0.05 are considered statistically significant.

Tissue microarrays used

Tissue microarrays used in this study were constructed as described in the work of Cox and colleagues (26). Gleason microarray contains tissue 1-mm cores from 88 patients with Gleason grade from 3 to 5 spotted in duplicate (176 cores total). Castrate-resistant prostate cancer (CRPC) array contains 1-mm cores from 12 patients with CRPC spotted in duplicate (24 cores in total).

DNA sequencing

Sequencing of the original urethra tumor specimen used for LTL352 xenograft was conducted at BCCA Genome Sciences Centre in Vancouver, British Columbia, Canada according to established protocols as described in the work of Shah and colleagues (27). Approximately 100 million reads were obtained and mapped to the National Center for Biotechnology Information 36.1 human genome reference sequence using MAQ 0.7.1 (28) and the following parameters: -n 1 -N -e 100 −a 700. The total number of sequenced bases in a given genomic window and the average sequencing depth across the window (10 or 30 kb) was then calculated. The copy number was approximated by the ratio of average sequencing depth in a given window to the average sequencing depth across the genome. This value was transformed into log2 space. Copy number profiles were visualized and copy number abnormalities associated with resistance phenotype identified using the NexusCGH software package (Biodiscovery Inc.).

Array comparative genomic hybridization

Digestion of snap-frozen tumor tissue with 0.2 mg/mL Proteinase K (Roche) in digestion buffer (50 mmol/L NaCl, 10 mmol/L Tris-HCl (pH 8.3), 1 mmol/L EDTA, and 0.5% SDS) was carried out overnight at 55°C. The cell lysates were purified by phenol:chloroform:isoamyl alcohol (25:24:1), and DNA was precipitated by adding 1/10th volume of 3 mol/L sodium acetate and 2.5 volumes of 100% ethanol at −20°C. The DNA was resuspended in water at 37°C for 1 hour. A total of 0.5 μg of tumor and male reference genomic DNA (Promega Corp.) was fluorescently labeled by following the NimbleGen enzymatic labeling protocol that uses Cy3- and Cy5-labeled random nanomers (TriLink Biotechnologies), a heat fragmentation step at 98°C for 10 minutes, and amplification with Klenow fragment 5′-3′exo- (NEB). Five micrograms of each Cy5-labeled sample was cohybridized with 5 μg of Cy3-labeled human male reference DNA (Promega Corp.) on Agilent SurePrint G3 Human Catalog CGH 4 × 180K (part no. G4449A), following the hybridization and washing conditions from the Agilent Oligonucleotide Array-Based CGH for Genomic DNA Analysis Protocol v6.2. Arrays were scanned with the Agilent DNA Microarray Scanner and quantified with the Feature Extraction 10.5.1.1. Comparative genomic hybridization (CGH) processed signal was then uploaded into Biodiscovery Nexus CGH v.5.1 software where the quality was assessed and data were visualized and analyzed.

Published OnlineFirst January 17, 2012; DOI:10.1158/1535-7163.MCT-11-0826

Results

Small cell carcinoma of the prostate expressing neuroendocrine markers

A 77-year-old Caucasian male patient (#946) was diagnosed with a metastatic prostatic adenocarcinoma with a Gleason score of 5 + 4 = 9. At the time of diagnosis, his serum PSA level was 14 ng/mL. The patient was treated with continuous androgen ablation therapy (Zoladex and Casodex combination). Forty months later he developed, despite a good initial response, a large local recurrence and a bladder outlet obstruction and was treated with palliative radiotherapy. Tumor growth resumed within 2 months and the patient developed bleeding and urinary retention and underwent a palliative cystoprostatectomy. Pathology evaluation revealed poorly differentiated carcinoma extending into the seminal vesicle, bladder neck, and the right ureter. Two months later, and 4 years after his initial diagnosis, palpable metastatic lesions were excised from his bulbar urethra and corpora cavernosa showing extensive involvement of small cell carcinoma infiltrating smooth muscle with the expression of typical neuroendocrine markers, that is, CD56, chromogranin A, and synaptophysin (Fig. 1) and absence of expression of AR and TP63 (Supplementary Fig. S1).

Genome sequencing of patient's tumor identifies a 9p21 *MTAP-CDKN2A* deletion

In an effort to identify therapeutic strategies based on the genotype of this patient's tumor, we sequenced the genome of the urethral neuroendocrine metastasis using Illumina MPS (29). We converted approximately 100 million mapped paired-end sequence reads to copy number data and visualized the resulting copy number plots with Biodiscovery Nexus CGH software. This process revealed a highly rearranged tumor genome showing a homozygous deletion in chromosome 9p21 (Fig. 2). Inspection of the 9p21 deletion confirmed that it was homozygous and showed that it had a size of 450 kilobases and encompassed the *MTAP* and *CDKN2A* genes, as well as 2 other genes, that is, the doublesex and mab-3–related transcription factor 1 (*DMRTA1*) and the embryonic lethal, abnormal vision (*ELAVL2*) genes. Sequencing the transcriptome of the patient's neuroendocrine prostate cancer metastasis revealed that *MTAP* and *CDKN2A* transcripts could be detected but at very low levels, presumably reflecting a combination of infiltrating macrophages, tumor heterogeneity, and stromal admixture (Fig. 3).

Patient's tumor xenograft line has the same 9p21 *MTAP-CDKN2A* deletion

In parallel with DNA sequencing, a transplantable subrenal capsule xenograft line, LTL352, was successfully established from the patient's neuroendocrine urethral metastasis. The subrenal location for xenografts was chosen because our past experience showed that this grafting site is ideal for establishing patient-derived xenografts (25, 30–32). All the grafts started to grow after a latency period of about 3 months. The tumor volume doubling time of LTL352 in NOD/SCID mice was about 11 days. The phenotype of the original cancer was retained throughout the serial transplantations, as indicated by its histology and in particular by the expression of the neuroendocrine marker, synaptophysin (Fig. 1) and absence of expression of AR and TP63 (Supplementary Fig. S1). Furthermore, as shown by array CGH (aCGH), the LTL352 xenograft line had the same 9p21 *MTAP-CDKN2A* deletion as the patient's tumor (Fig. 2). LTL352 also had the lowest MTAP expression according to quantitative PCR (Fig. 3B).

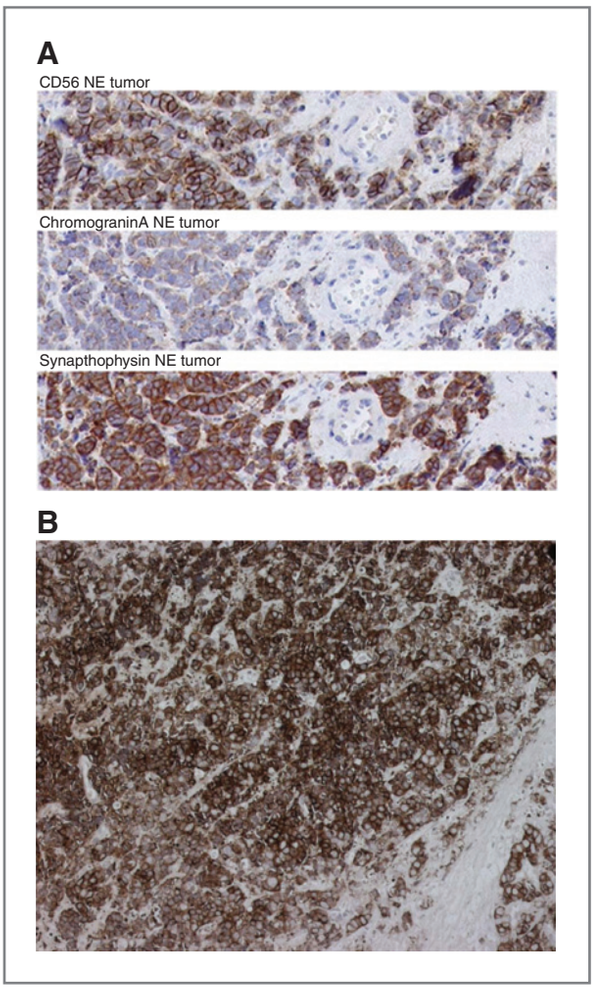

Figure 1. A, immunohistochemical staining of tumor 946 tissue sections shows expression of neuroendocrine markers CD56, chromogranin A, and synaptophysin, identifying the neuroendocrine origin of the tissue. B, synaptophysin staining of xenograft LTL352 tissue. NE, neuroendocrine.

Effect of 6-TG ± MTA treatment on LTL352 xenograft growth

Groups of NOD/SCID mice carrying subcutaneous LTL352 xenografts (size 100–160 mm^3) were treated (intraperitoneally) during a 12-day period (on days 1, 5, and 9)

Published OnlineFirst January 17, 2012; DOI:10.1158/1535-7163.MCT-11-0826

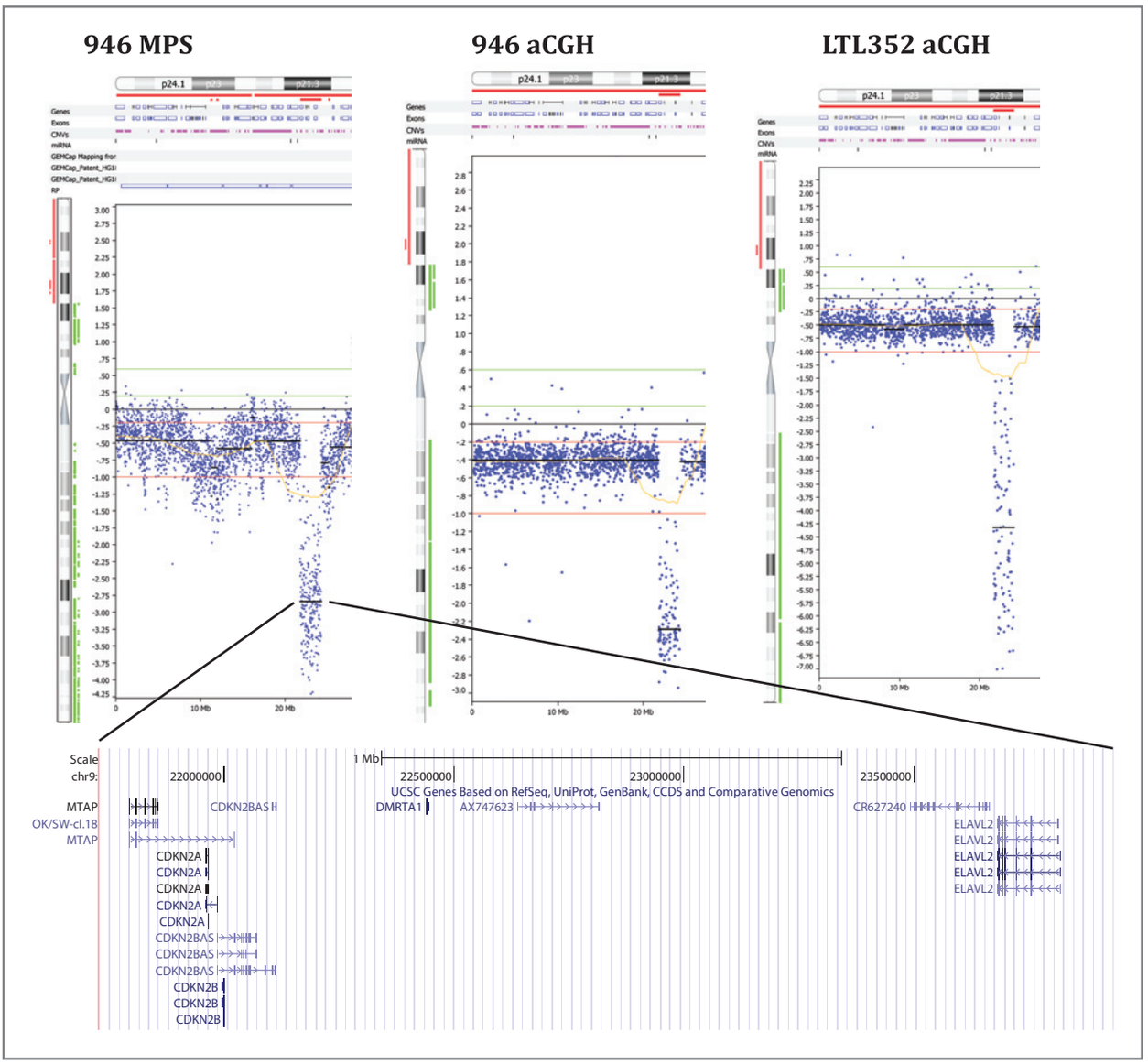

Figure 2. Comparison of chromosome 9p copy number profiles of the neuroendocrine urethra metastasis from patient #946 and its xenograft, LTL352, as produced by Illumina sequencing (MPS) and Agilent aCGH technologies. aCGH confirmed that the deletion in the original tumor by MPS was real and not a mapping artifact and that the patient's tumor and xenograft had the same deletion. Copy number profiles were visualized using NexusCGH (Biodiscovery, Inc.). The *MTAP* deletion is expanded in the bottom (University of California, Santa Cruz). Three additional genes mapping to this deletion are *CDKN2A*, *DMRTA1*, and *ELAVL2*.

with 6-TG (75 mg/kg, 7 mice), 6-TG + MTA (75 mg/kg and 100 mg/kg respectively, 7 mice), or saline (controls, 5 mice). As shown in Fig. 4A, the growth of the xenografts was markedly inhibited by 6-TG + MTA. In the control group, the average tumor volume increased over the 12-day period from 150 ± 22 to 315 ± 48 mm^3 (mean ± SEM)—an increase of about 110%. In the 6-TG + MTA group, the tumor volume increased only slightly from 134 ± 12 to 182 ± 18 mm^3—an increase of about 36%. This amounts to a (6-TG + MTA)-induced growth inhibition (the percentage increase of tumor volume of treated tumors compared with the controls) of 74% ($P < 0.05$). Administration of 6-TG on its own was highly toxic resulting in the death of all 6-TG–treated mice within 12 days, whereas none of the mice treated with 6-TG + MTA showed significant weight loss. Histopathologic analysis was used to determine the effect of the drugs at the cellular level. A comparison with the control tissues showed that the tissues of (6-TG + MTA)-treated tumors contained more apoptotic bodies (Fig. 4B). Furthermore, a marked increase was found for the staining of caspase-3 (a marker of apoptosis) for the (6-TG + MTA)-treated group (Fig. 4B)—6-TG + MTA xenografts had 4.49% ± 0.26% (mean ± SD) of caspase-3–positive cells—a highly

Published OnlineFirst January 17, 2012; DOI:10.1158/1535-7163.MCT-11-0826

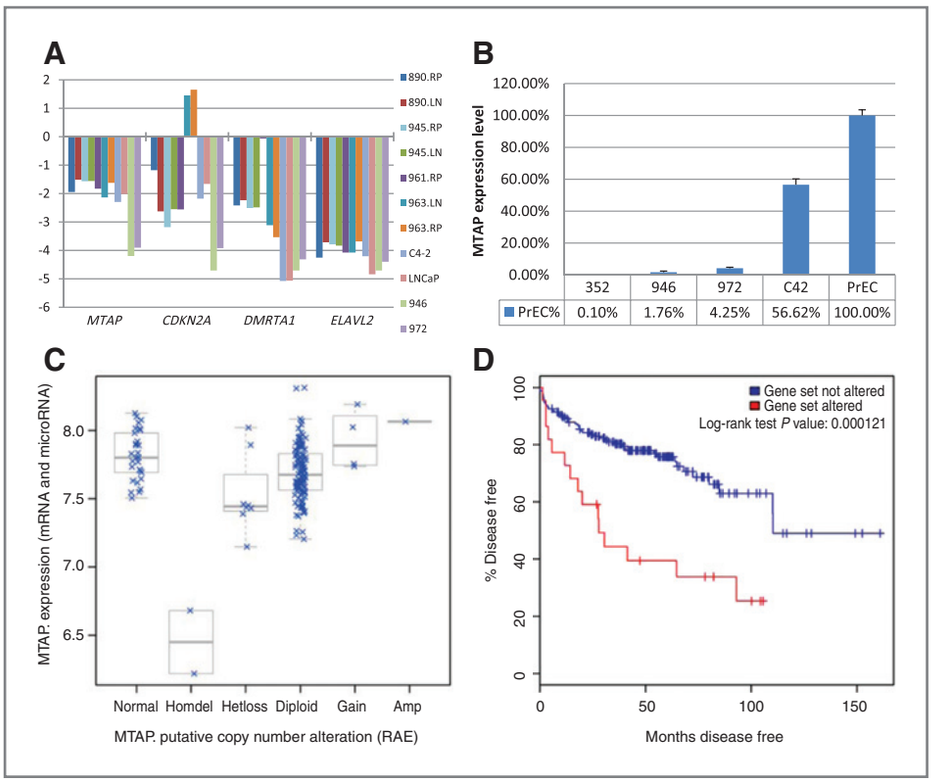

Figure 3. Expression of genes mapping within the 9p21 *MTAP* deletion. A, RNA sequence-derived expression data for *MTAP*, *CDKN2A*, *DMRTA1*, and *ELAVL2*—genes located within the minimal deletion at the *MTAP* locus. Expression levels were normalized to glyceraldehyde-3-phosphate dehydrogenase (GAPDH). All samples had normal copy numbers of the *MTAP* locus with the exception of 946 and 972 urethra and penile metastases, respectively. Only the expression of *MTAP* shows essentially perfect correlation with the copy number. B, quantitative RT-PCR was carried out to confirm this interpretation of the RNA sequence data and to confirm concordance between 946 and 352. C, *MTAP* expression levels determined in a Sloan–Kettering prostate cancer cohort (35). The cBio Cancer Genomics Portal was used for data access (http://www.cbioportal.org/cgx/?cancer_type_id = pca). The *MTAP* expression levels correlate well with the reduced copy numbers of *MTAP* locus. D, Kaplan–Meier plot showing differences in time to recurrence as measured by PSA for the 26 patients with *MTAP* expression differing from the mean by a *Z*-score of 2.0 or greater compared with the rest of the cohort. Decreased *MTAP* expression is significantly correlated with a shorter time to disease recurrence.

significant ($P < 0.0001$) increase over the control group's 1.42% ± 0.17% (mean ± SD)—in line with reported induction of apoptosis by 6-TG (33). Also, Ki-67 activity (a marker of cell proliferation) was reduced in the (6-TG + MTA)-treated tumors ($P < 0.01$, data not shown) compared with the control group. Taken together, the results indicate that addition of MTA to 6-TG was effective in protecting the host from 6-TG toxicity thus enhancing specific targeting of the malignancy.

It should be noted that the choice of 12-day study duration was prompted by 2 considerations. First, the doubling time of LTL352 is approximately 11 days. Second, the approved animal protocol limits the final sum of tumor volume in the mouse by 1,000 mm^3. Therefore, we had to ensure, that the volume of each graft would not exceed 350 mm^3, as there are 2 to 3 grafts per mouse.

We have sequenced the genomes of 20 high-risk prostate tumors at the Vancouver Prostate Centre and found *MTAP* to be deleted in 30% of them. In independent cohorts analyzed by Affymetrix SNP arrays, *MTAP* was found to be deleted in 10% (3 of 30) and 70% (5 of 7) of prostatic adenocarcinomas and neuroendocrine tumors, respectively. Finally, we find *MTAP* deletion to occur significantly ($P = 0.027$, the Fisher exact test) more often in CRPC tumor samples on a Vancouver Prostate Centre CRPC tissue microarray (3 out of 12 patients have deletions) compared with Gleason 2009 array (where deletion was detected in 2 of 78 patients). We also find *MTAP* to be significantly ($P = 0.036$, the Fisher exact test) more often deleted in GEO GSE14996 data set that contains Affymetrix SNP6.0–based copy number profiles of multi-sampled metastatic prostate tumors (ref. 34; 3 of 14 patients have deletions) compared with Vancouver Prostate Centre Gleason 2009 tissue microarray. In the majority of these tumors, *MTAP* is heterozygously deleted and *MTAP* expression correlates well with copy number (Fig. 3C). To understand the clinical significance of this, we analyzed gene expression data for 230 prostate tumors (accessible at cBio Cancer Genomics Portal developed by the Computational Biology Center at Memorial Sloan-Kettering Cancer Center, New York; ref. 35) and found that *MTAP* expression is decreased by more than 2

Published OnlineFirst January 17, 2012; DOI:10.1158/1535-7163.MCT-11-0826

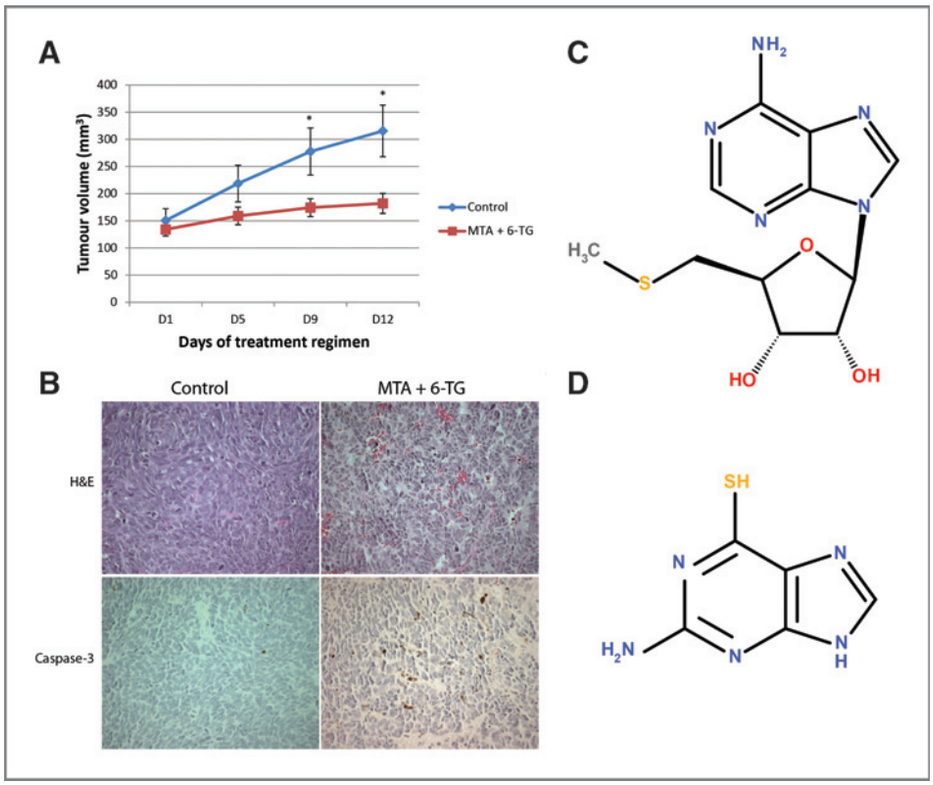

Figure 4. A, mice carrying LTL352 xenografts were treated (intraperitoneally) with 6-TG (75 mg/kg) + MTA (100 mg/kg) or saline (controls) on days 1, 5, and 9. On day 12, the tumors in the treated group were approximately 64% smaller than those in the untreated control group (a decrease of tumor growth rate by about 74%). Mean values with SEM are plotted. *, significant differences between control and treated tumors (paired *t* test, $P < 0.05$). All mice treated with 6-TG in the absence of MTA died within 12 days. B, histologic and immunohistochemical analysis of LTL352 tissues from control (untreated) and 6-TG + MTA-treated xenografts. Representative fields of H&E and caspase-3 staining are shown. In the treated mice, the tumors had reduced proliferation and increased apoptosis when compared with the control tumors as illustrated by increase of caspase-3–positive cells from 1.42% ± 0.17% to 4.49% ± 0.26% (mean ± SD). C, the chemical structure of MTA. D, the chemical structure of 6-TG.

Z-scores in approximately 11% of tumors. Moreover, a Kaplan–Meier analysis revealed that *MTAP* expression is associated with significantly shorter time to postoperative recurrence as measured by PSA (Fig. 3D). Thus, reduced expression of *MTAP* seems to be both prognostic and predictive for *MTAP*-based therapies.

Discussion

To gain insight into the molecular mechanisms driving prostate tumor progression, and to devise novel therapeutic strategies, we routinely sequence prostate tumor genomes and/or transcriptomes from selected patients. This approach led to the finding that the neuroendocrine small cell carcinoma presented in this study had a homozygous *MTAP-CDKN2A* deletion as shown by MPS and confirmed by aCGH (Fig. 2). The absence of *MTAP* in the tumor motivated experimentation to determine whether it might respond to a therapeutic strategy first advanced by Lubin and Lubin (15), based on use of a high dose of a purine analogue, such as 6-TG, in combination with MTA. In normal host cells this combination competitively inhibits conversion of 6-TG to its toxic nucleotide and as such can protect the host from 6-TG toxicity. But in MTAP-deficient tumor cells, MTA does not protect the tumor from 6-TG toxicity, and the tumor is inhibited or is killed. This selective strategy was previously found to be effective for treatment of the human T-cell leukemia, CCRF-CEM, in a mouse xenograft model, whereas the host mouse tissues were protected by MTA from 6-TG toxicity (13).

Development of new drugs has been seriously hampered by the lack of clinically relevant, experimental *in vivo* cancer models required for drug efficacy evaluation. Only about 5% of potential new anticancer agents, that have successfully passed all required preclinical tests, have efficacy in clinical trials and are approved for clinical usage by the U.S. Food and Drug Administration (36). There is, therefore, a critical need for experimental models with improved ability to predict clinical drug efficacy (37). To overcome this hurdle, we have recently developed transplantable, patient-derived tumor tissue xenografts that have very high engraftment rates (>95%) in NOD/SCID mice and closely resemble the original cancers in histopathology, biomarker expression, and genetic profiles (25, 32, 38–41). The LTL352 subrenal capsule xenograft line established from the patient's tumor closely resembles the patient's tumor particularly with regard to expression of the neuroendocrine marker, synaptophysin (Fig. 1), and the 9p21 *MTAP-CDKN2A* deletion (Fig. 2). That the 6-TG + MTA treatment indeed had an inhibitory effect on the solid tumor xenografts that was showed by the marked reduction in their growth rate (Fig. 4A), by decreases in Ki-67 expression (data not shown) and increases in caspase-3 expression and apoptotic bodies in the cancer cells (Fig. 4B). The protective effect of MTA was evident from the lack of weight loss of the (6-TG + MTA)-treated mice in contrast to the 6-TG–treated mice

Published OnlineFirst January 17, 2012; DOI:10.1158/1535-7163.MCT-11-0826

for which treatment with 6-TG, in the absence of MTA, was lethal.

While further optimization of dose and scheduling is needed to increase the growth inhibitory effect, these studies show clearly that significant *in vivo* growth inhibition of *MTAP*-deficient solid tumors can be obtained, without toxicity to the host, by using 6-TG in combination with MTA. This combination therapy should be especially useful for cancers without effective therapy. As MTA has been given safely to humans, we are planning clinical trials using this strategy in patients with tumors lacking *MTAP*. Unfortunately, in the case of the tissue donor for this study, he continued to require palliative treatments for local and metastatic progression over the following 18 months before dying of metastatic prostate cancer.

To our knowledge, this is the first study to directly implicate loss of *MTAP* in prostate cancer and to associate it with the invariably fatal CRPC. Moreover, this is one of the first studies to exploit whole-genome sequencing for identification of a molecular target in a patient's tumor in conjunction with *in vivo* evaluation of the target-related therapy using a patient-derived xenograft of the patient's cancer. The latter could be especially useful for personalized cancer therapy.

Disclosure of Potential Conflicts of Interest

M. Lubin has filed a patent application for using MTA/6-TG therapy in MTAP-deficient tumors. No potential conflicts of interest were disclosed by the other authors.

Grant Support

This study was supported by the Canadian Institutes of Health Research (Y.Z. Wang/M. Gleave) Centres of Excellence for Commercialization and Research (M. Gleave), and PNW Prostate SPORE P50 CA097186, Prostate Cancer Canada, and Genome BC (C.C. Collins). Y.Z. Wang is a recipient of an Overseas Chinese Scholar Award from the National Natural Science Foundation of China (30928027) and a recipient of an Innovative Scholar Award from ICARE. The work in laboratory of A. M. Chinnaiyan was supported by NIH P50 CA69568, U01 CA111275, and R01CA132874 grants.

The costs of publication of this article were defrayed in part by the payment of page charges. This article must therefore be hereby marked *advertisement* in accordance with 18 U.S.C. Section 1734 solely to indicate this fact.

Received October 13, 2011; revised December 13, 2011; accepted December 27, 2011; published OnlineFirst January 17, 2012.

References

1. di Sant'Agnese PA. Neuroendocrine differentiation in carcinoma of the prostate. Diagnostic, prognostic, and therapeutic implications. Cancer 1992;70:254–68.
2. Abbas F, Civantos F, Benedetto P, Soloway MS. Small cell carcinoma of the bladder and prostate. Urology 1995;46:617–30.
3. Randolph TL, Amin MB, Ro JY, Ayala AG. Histologic variants of adenocarcinoma and other carcinomas of prostate: pathologic criteria and clinical significance. Mod Pathol 1997;10:612–29.
4. Erasmus CE, Verhagen WI, Wauters CA, van Lindert EJ. Brain metastasis from prostate small cell carcinoma: not to be neglected. Can J Neurol Sci 2002;29:375–7.
5. Miyoshi Y, Uemura H, Kitami K, Satomi Y, Kubota Y, Hosaka M. Neuroendocrine differentiated small cell carcinoma presenting as recurrent prostate cancer after androgen deprivation therapy. BJU Int 2001;88:982–3.
6. Tanaka M, Suzuki Y, Takaoka K, Suzuki N, Murakami S, Matsuzaki O, et al. Progression of prostate cancer to neuroendocrine cell tumor. Int J Urol 2001;8:431–6; discussion 437.
7. Papandreou CN, Daliani DD, Thall PF, Tu SM, Wang X, Reyes A, et al. Results of a phase II study with doxorubicin, etoposide, and cisplatin in patients with fully characterized small-cell carcinoma of the prostate. J Clin Oncol 2002;20:3072–80.
8. Spieth ME, Lin YG, Nguyen TT. Diagnosing and treating small-cell carcinomas of prostatic origin. Clin Nucl Med 2002;27:11–7.
9. Abrahamsson PA. Neuroendocrine differentiation in prostatic carcinoma. Prostate 1999;39:135–48.
10. Bonkhoff H. Neuroendocrine cells in benign and malignant prostate tissue: morphogenesis, proliferation, and androgen receptor status. Prostate Suppl 1998;8:18–22.
11. Helpap B. Morphology and therapeutic strategies for neuroendocrine tumors of the genitourinary tract. Cancer 2002;95:1415–20.
12. Moore SR, Reinberg Y, Zhang G. Small cell carcinoma of prostate: effectiveness of hormonal versus chemotherapy. Urology 1992;39:411–6.
13. Bertino JR, Waud WR, Parker WB, Lubin M. Targeting tumors that lack methylthioadenosine phosphorylase (MTAP) activity: current strategies. Cancer Biol Ther 2011;11:627–32.
14. Marce S, Balague O, Colomo L, Martinez A, Holler S, Villamor N, et al. Lack of methylthioadenosine phosphorylase expression in mantle cell lymphoma is associated with shorter survival: implications for a potential targeted therapy. Clin Cancer Res 2006;12:3754–61.
15. Lubin M, Lubin A. Selective killing of tumors deficient in methylthioadenosine phosphorylase: a novel strategy. PLoS One 2009;4:e5735.
16. Krasinskas AM, Bartlett DL, Cieply K, Dacic S. CDKN2A and MTAP deletions in peritoneal mesotheliomas are correlated with loss of p16 protein expression and poor survival. Mod Pathol 2010;23:531–8.
17. Basu I, Cordovano G, Das I, Belbin TJ, Guha C, Schramm VL. A transition state analogue of 5′-methylthioadenosine phosphorylase induces apoptosis in head and neck cancers. J Biol Chem 2007;282:21477–86.
18. Basu I, Locker J, Cassera MB, Belbin TJ, Merino EF, Dong X, et al. Growth and metastases of human lung cancer are inhibited in mouse xenografts by a transition state analogue of 5′-methylthioadenosine phosphorylase. J Biol Chem 2011;286:4902–11.
19. Christopher SA, Diegelman P, Porter CW, Kruger WD. Methylthioadenosine phosphorylase, a gene frequently codeleted with p16 (cdkN2a/ARF), acts as a tumor suppressor in a breast cancer cell line. Cancer Res 2002;62:6639–44.
20. Kirovski G, Stevens AP, Czech B, Dettmer K, Weiss TS, Wild P, et al. Down-regulation of methylthioadenosine phosphorylase (MTAP) induces progression of hepatocellular carcinoma via accumulation of 5′-deoxy-5′-methylthioadenosine (MTA). Am J Pathol 2011;178:1145–52.
21. Clurman BE, Groudine M. The CDKN2A tumor-suppressor locus–a tale of two proteins. N Engl J Med 1998;338:910–2.
22. Huang HY, Li SH, Yu SC, Chou FF, Tzeng CC, Hu TH, et al. Homozygous deletion of MTAP gene as a poor prognosticator in gastrointestinal stromal tumors. Clin Cancer Res 2009;15:6963–72.
23. Behrmann I, Wallner S, Komyod W, Heinrich PC, Schuierer M, Buettner R, et al. Characterization of methylthioadenosin phosphorylase (MTAP) expression in malignant melanoma. Am J Pathol 2003;163:683–90.
24. Kindler HL, Burris HA III, Sandler AB, Oliff IA. A phase II multicenter study of L-alanosine, a potent inhibitor of adenine biosynthesis, in patients with MTAP-deficient cancer. Invest New Drugs 2009;27:75–81.
25. Wang Y, Revelo MP, Sudilovsky D, Cao M, Chen WG, Goetz L, et al. Development and characterization of efficient xenograft models for benign and malignant human prostate tissue. Prostate 2005;64:149–59.

Published OnlineFirst January 17, 2012; DOI:10.1158/1535-7163.MCT-11-0826

26. Cox ME, Gleave ME, Zakikhani M, Bell RH, Piura E, Vickers E, et al. Insulin receptor expression by human prostate cancers. Prostate 2009;69:33–40.

27. Shah SP, Morin RD, Khattra J, Prentice L, Pugh T, Burleigh A, et al. Mutational evolution in a lobular breast tumour profiled at single nucleotide resolution. Nature 2009;461:809–13.

28. Li H, Ruan J, Durbin R. Mapping short DNA sequencing reads and calling variants using mapping quality scores. Genome Res 2008;18: 1851–8.

29. Zhao J, Grant SF. Advances in whole genome sequencing technology. Curr Pharm Biotechnol 2011;12:293–305.

30. Lin D, Watahiki A, Bayani J, Zhang F, Liu L, Ling V, et al. ASAP1, a gene at 8q24, is associated with prostate cancer metastasis. Cancer Res 2008;68:4352–9.

31. Tung WL, Wang Y, Gout PW, Liu DM, Gleave M. Use of irinotecan for treatment of small cell carcinoma of the prostate. Prostate 2011;71: 675–81.

32. Wang Y, Xue H, Cutz JC, Bayani J, Mawji NR, Chen WG, et al. An orthotopic metastatic prostate cancer model in SCID mice via grafting of a transplantable human prostate tumor line. Lab Invest 2005;85: 1392–404.

33. Karran P, Attard N. Thiopurines in current medical practice: molecular mechanisms and contributions to therapy-related cancer. Nat Rev Cancer 2008;8:24–36.

34. Liu W, Laitinen S, Khan S, Vihinen M, Kowalski J, Yu G, et al. Copy number analysis indicates monoclonal origin of lethal metastatic prostate cancer. Nat Med 2009;15:559–65.

35. Taylor BS, Schultz N, Hieronymus H, Gopalan A, Xiao Y, Carver BS, et al. Integrative genomic profiling of human prostate cancer. Cancer Cell 2010;18:11–22.

36. Sharpless NE, Depinho RA. The mighty mouse: genetically engineered mouse models in cancer drug development. Nat Rev Drug Discov 2006;5:741–54.

37. Voskoglou-Nomikos T, Pater JL, Seymour L. Clinical predictive value of the *in vitro* cell line, human xenograft, and mouse allograft preclinical cancer models. Clin Cancer Res 2003;9:4227–39.

38. Lee CH, Xue H, Sutcliffe M, Gout PW, Huntsman DG, Miller DM, et al. Establishment of subrenal capsule xenografts of primary human ovarian tumors in SCID mice: potential models. Gynecol Oncol 2005;96: 48–55.

39. Cutz JC, Guan J, Bayani J, Yoshimoto M, Xue H, Sutcliffe M, et al. Establishment in severe combined immunodeficiency mice of subrenal capsule xenografts and transplantable tumor lines from a variety of primary human lung cancers: potential models for studying tumor progression-related changes. Clin Cancer Res 2006;12: 4043–54.

40. Andersen RJ, Mawji NR, Wang J, Wang G, Haile S, Myung JK, et al. Regression of castrate-recurrent prostate cancer by a small-molecule inhibitor of the amino-terminus domain of the androgen receptor. Cancer Cell 2010;17:535–46.

41. Kortmann U, McAlpine JN, Xue H, Guan J, Ha G, Tully S, et al. Tumor growth inhibition by olaparib in BRCA2 germline-mutated patient-derived ovarian cancer tissue xenografts. Clin Cancer Res 2011;17: 783–91.